INTERNATIONAL JOURNAL FOR NUMERICAL METHODS IN FLUIDS, VOL. 4, 71–97 (1984)

SELECTIVE LUMPING FINITE ELEMENT METHOD FOR NEARSHORE CURRENT*

MUTSUTO KAWAHARA AND KAZUO KASHIYAMA

Department of Civil Engineering, Chuo University Kasuga, Bunkyo-ku, Tokyo, 112, Japan

SUMMARY

A finite element method for the analysis of nearshore current, which is one of the principal currents in coastal seas, is presented in this paper. Because the nearshore current is induced by the variable distribution of the surface waves, it is necessary to analyse two main characteristics of the wave, i.e. direction and height. The current can be computed using the resulting wave characteristics. The present method makes it possible to employ procedures for which the same methods of solution are applicable for all basic equations of wave direction, height and current flow. The linear interpolation function is used for the discretization of spatial variables and a selective lumping two step explicit scheme is employed for the numerical integration in time. The numerical solutions obtained are compared with analytical, experimental and observed ones. From these comparative studies, it is concluded that the present finite element method provide a useful tool for the analysis of nearshore current.

KEYWORDS Nearshore Current Two Step Explicit Scheme Linear Interpolation Function Fujisawa Coast

INTRODUCTION

In a coastal sea near a beach, the variation of the surface wave distribution becomes extraordinally complicated and irregularly variable. Moreover, waves can occur which break near a coast after having passed through the breaking point. The surface waves in coastal seas generate a considerable high velocity current in a direction toward, outward or alongside a beach. The current induced by the variable distribution of the waves is generally referred to as the nearshore current.[1–6] The velocity of the nearshore current is sometimes almost the same order as those of tidal current, wind drift current and so on. In a coastal sea near a beach, where the water depth becomes shallower, the sea bottom topography and coastal geometry greatly affect the current flow. Therefore, it is quite necessary and important to develop a flexible finite element method, to consider the bottom topography and coastal geometry.

The finite element method, in which velocity and water elevation are taken as the field variables to solve steady flow, was presented by Skovgaard and Jonsson.[7] In their analysis, the wave distribution was determined according to the conventional formulation of conservation of waves. A linear interpolation function is used for velocity and a quadratic interpolation function for water elevation. Liu and Lennon[8] discussed the finite element method based on the stream function method dealing with wave diffraction by the ray method. The finite element analysis based on the isoparametric element is investigated by Bettess *et al.*,[9]

* This invited paper is an extended and refereed version of one presented at the Fourth International Symposium on Finite Elements in Flow Problems held in Tokyo, Japan, July 26–29, 1982.

0271–2091/84/010071–27$02.70 *Received 16 May 1983*
© 1984 by John Wiley & Sons, Ltd.

who employed the Helmholz equation to determine the wave field. Wu and Liu[10] presented the steady flow analysis considering eddy viscosity and bottom friction by the conventional direct method. Kawahara *et al.*,[11] and Kawahara and Takagi[12] published the finite element method based on the stream function formulation. The wave angle is computed by a non-linear incremental iteration method. Kawahara *et al.*[13] discussed the method based on the conservations of wave number and wave energy, the equation of motion and the equation of continuity. However, the coupling effects are ignored.

This paper presents the finite element method for the determination of surface wave direction, wave height and current flow. Contrary to the method previously published, the present method employs the same finite element procedures for all equations of wave and current. The conservation equations of wave number and energy are used to determine the wave. For the current flow, equations of motion and continuity, including radiation stress, are employed. It can be made possible to transform all the basic equations to first order differential equations. This enables the time marching finite element method, especially the explicit method, to be effectively used. Because the basic equations are non-linear and field variables are coupled to each other, iterative computations are necessary to solve these equations. For this purpose, the following procedures are used. At first, assuming the flow field, the wave direction is solved. Using the flow and the computed wave direction, the wave height is determined. Then, employing the resulting wave direction and height, the current flow can be obtained. The iteration cycle is repeated until a steady current flow is determined.

Following the standard Galerkin finite element procedure the weighted residual equation is derived for all basic equations. A linear polynomial function based on a three node triangular finite element is employed for the interpolation of wave number, wave height, current flow and water elevation. The fact that the same linear interpolation function can be used for all field variables greatly reduces the computational effort compared with the conventional analysis. In recent papers, Kawahara *et al.*[14] have shown that the selective lumping two step explicit method is useful for the computation of transient shallow water flow. Several numerical examples have been carried out to illustrate the adaptability of the present finite element method.

As a numerical test example, the wave direction, wave height, and current flow are compared with the analytical solution ignoring the coupling effect. Numerical results are compared with the experimental results obtained by Mizuguchi *et al.*[15,16] All the comparisons are in extremely good agreement. Numerical computations have been carried out for the coastal current at the Fujisawa Coast. The rip current zones computed are closely related to the zone obtained by observation.[17] It is concluded that the finite element method presented in this paper is a successful tool for the analysis of transient nearshore current flow.

BASIC EQUATIONS

A Cartesian co-ordinate system is introduced in which the x-axis is placed normal to the coastline and the y-axis is placed parallel to it as shown in Figure 1. The nearshore current is that which is induced by the variable distribution of wave energy around the surf zone near a sea coast. Thus, it is strictly necessary to describe the surface wave distribution. In this paper, a wave theory which is based on trains of long, smooth, regular waves is employed, although actual sea waves are frequently short-ceased, random and irregular. These sorts of irregularity can be modelled by the superposition of regular waves with various frequencies. The waves are specified by two main characteristic quantities, wave direction and wave height.

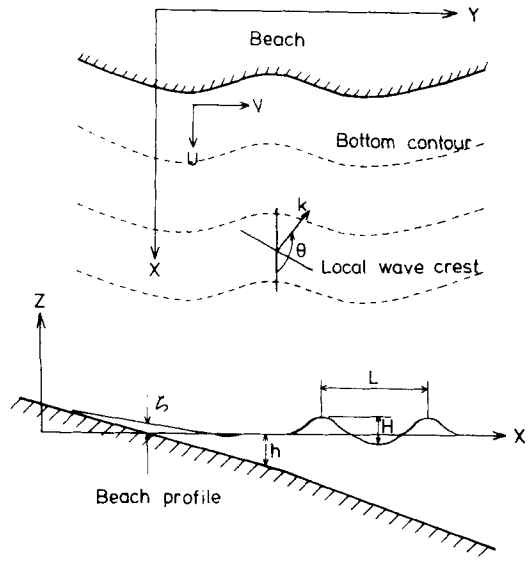

Figure 1. Co-ordinate system

These are actually described by the equations of conservation. The nearshore current is expressed by the conservations of momentum and continuity, postulating the concept of radiation stress.[1–6] The fluid is assumed to be transient, incompressible and turbulent. The vertical component of the current is neglected and the mass current is assumed to be constant over the depth. Coriolis force and wind action are ignored. In this paper, all equations are expressed using the indicial notation and the usual summation convention with repeated indices.

Wave direction

The instantaneous wave form Z is expressed in general in the form:

$$Z = A \exp(i\chi) \tag{1}$$

where A is the local amplitude which determines the wave height and χ is the phase function, which is related to the wave direction. The imaginary unit is denoted by i. The functions A and χ are slowly varying functions of position and time. Wavenumber k and radian frequency n can be defined in terms of the phase function.

$$k_i = \chi_{,i} \tag{2}$$

$$n = -\frac{\partial \chi}{\partial t} \tag{3}$$

$$k = \sqrt{(k_i k_i)} \tag{4}$$

where k_i denotes the components of wavenumber which are related to the wave direction by

$$k_x = k \cos\theta, \qquad k_y = k \sin\theta \tag{5), (6}$$

where θ is the wave direction angle as shown in Figure 1. Combining equations (2) and (3),

the kinematical conservation equation can be derived as follows.

$$\frac{\partial k_i}{\partial t} + n_{,i} = 0 \tag{7}$$

considering the interaction between surface wave and current velocity u_i, the radian frequency n is given by

$$n = \sigma + k_i u_i \tag{8}$$

where n is called the observed frequency and σ is the intrinsic frequency. The frequency σ is derived from the dispersion relation:

$$\sigma^2 = gk \tanh k(h+\zeta) \tag{9}$$

where ζ denotes the water elevation, g and h are gravity acceleration and water depth, respectively. From equations (7) and (8), the following is obtained:

$$\frac{\partial k_i}{\partial t} + (\sigma + k_j u_j)_{,i} = 0 \tag{10}$$

Because σ is a function of wavenumber k and water depth h, equation (10) can be reformulated as follows.

$$\frac{\partial k_i}{\partial t} + \left(\frac{\partial \sigma}{\partial k_j}\right) k_{j,i} + \left(\frac{\partial \sigma}{\partial h}\right) h_{,i} + k_j u_{j,i} + u_j k_{j,i} = 0 \tag{11}$$

From equation (2), the irrotational condition on the wavenumber can be written as:

$$\varepsilon_{ij} k_{i,j} = 0 \tag{12}$$

where ε_{ij} is the Eddington's epsilon function. Introducing equation (9) into equation (11), using equation (12) and rearranging the terms, the kinematical conservation equation can be written in the following form.

$$\frac{\partial k_i}{\partial t} + C_{gj} k_{i,j} + f h_{,i} + k_j u_{j,i} + u_j k_{i,j} = 0 \tag{13}$$

where C_g is the group velocity,

$$C_{gj} = \frac{\partial \sigma}{\partial k_j} = \frac{1}{2} C_j \left\{ 1 + \frac{2k(h+\zeta)}{\sinh 2k(h+\zeta)} \right\} \tag{14}$$

in which C is the wave velocity:

$$C = \sqrt{\left[\left(\frac{g}{k} \right) \tanh k(h+\zeta) \right]} \tag{15}$$

and f is the gradient of frequency, which is expressed as follows:

$$f = \frac{\partial \sigma}{\partial h} = \frac{gk^2}{2\sigma} \operatorname{sech}^2 k(h+\zeta) \tag{16}$$

Using the resulting k_i, the wave angle θ can be calculated from equations (5) and (6)

$$\theta = \tan^{-1} \left(\frac{k_x}{k_y} \right) \tag{17}$$

As the boundary condition, the wave angle is described on the ocean-side boundary using the wave direction of the incident wave.

Wave height

The wave height distribution can be determined by the conservation law of wave energy, which is introduced by Longuet-Higgins and Stewart.[1-6] An equation for the balance of total energy can be expressed by

$$\frac{\partial}{\partial t}\int_{-h}^{\zeta} \rho(\tfrac{1}{2}\tilde{u}_i\tilde{u}_i + gz)\,dz + \left[\int_{-h}^{\zeta} \tilde{u}_j(\tfrac{1}{2}\rho\tilde{u}_k\tilde{u}_k + \rho gz + p)\,dz\right]_{,j} = 0 \tag{18}$$

where $\tilde{u}_i$ and p express total velocity and pressure, and ρ is the density of water. Assuming that the total velocity consists of current velocity u_i and wave velocity u_i', equation (18) can be reformulated to lead to the conservation equation of wave energy.

$$\frac{\partial E}{\partial t} + [E(C_{gi} + u_i)]_{,i} + S_{ij}u_{i,j} = 0 \tag{19}$$

where E denotes wave energy per unit surface area,

$$E = \tfrac{1}{8}\rho g H^2 \tag{20}$$

in which H represents wave height, being the ensemble average of wave height. Radiation stress is denoted by S_{ij}, which is defined as the excess momentum of the wave velocity and pressure, and will be expressed in equation (27).

The wave breaking height is determined by the following empirical equation,

$$H_b = \gamma h_b \tag{21}$$

where H_b and h_b represent wave breaking height and the water depth at which wave breaking occurs, respectively, and γ is an empirical constant lying between 0·6 and 1·0. On the shore zone between the beach and the breaking point, the broken wave height is assumed to be proportional to the water depth as:

$$H = \gamma h \tag{22}$$

As the boundary condition, the wave height is specified on the ocean-side boundary using the data of the incident wave.

Nearshore current

The nearshore current is normally induced by the unbalanced distribution of wave direction and energy. The current can be described by the conservation equations of momentum and continuity, vertically integrated assuming a hydrostatic pressure distribution, as

$$\int_{-h}^{\zeta} \left(\tilde{u}_{i,i} + \frac{\partial \tilde{w}}{\partial z}\right) dz = 0 \tag{23}$$

$$\frac{\partial}{\partial t}\int_{-h}^{\zeta} (\rho\tilde{u}_i)\,dz + \left[\int_{-h}^{\zeta} (\rho\tilde{u}_i\tilde{u}_j + p\delta_{ij})\,dz\right]_{,j} + \rho g(h+\zeta)\zeta_{,i} - \tau_i = 0 \tag{24}$$

where $\tilde{w}$ is vertical velocity, τ_i means viscosity and friction terms and δ_{ij} is the delta function. Equations (23) and (24) lead to the conservation equations in which the unknown variables

are mean velocity u_i and water elevation ζ.

$$\frac{\partial u_i}{\partial t}+u_j u_{i,j}+\frac{1}{\rho(h+\zeta)}S_{ij,j}+g\zeta_{,i}-A_l(u_{i,j}+u_{j,i})_{,j}+\frac{f_c}{(h+\zeta)}u_i=0 \tag{25}$$

$$\frac{\partial \zeta}{\partial t}+\{(h+\zeta)u_i\}_{,i}=0 \tag{26}$$

where radiation stress S_{ij} is expressed as

$$S_{ij}=\int_{-h}^{\zeta}(\overline{\rho u_i' u_i'}+\bar{p}\delta_{ij})\,dz-\frac{\rho g}{2}(h+\zeta)^2\delta_{ij}+\frac{\rho g}{2}\bar{\zeta}'^2\delta_{ij} \tag{27}$$

in which u_i' is the velocity fluctuation due to the wave, p is the pressure including fluctuation and an overbar represents an ensemble average. The normal wave potential has the form:

$$\phi=\frac{nA}{k}\frac{\cosh k(z+\zeta)}{\sinh k(h+\zeta)}\sin(k_i x_i-nt) \tag{28}$$

Using this, the fluctuations of wave height ζ', velocity u_i', and velocity in the direction of water depth w' can be derived in the form:

$$\zeta'=A\cos(k_i x_i-nt) \tag{29}$$

$$u_i'=\frac{nA\cosh k(z+h)}{\sinh k(h+\zeta)}\left(\frac{k_i}{k}\right)\cos(k_i x_i-nt) \tag{30}$$

$$w'=\frac{nA\sinh k(z+h)}{\sinh k(h+\zeta)}\sin(k_i x_i-nt) \tag{31}$$

Introducing equations (29)–(31) into equation (27) and rearranging the terms, the following form of the radiation stress can be derived:

$$S_{ij}=E\left(\frac{C_g}{C}\right)l_i l_j+\frac{E}{2}\left(\frac{2C_g}{C}-1\right)\delta_{ij} \tag{32}$$

where

$$l_i=\frac{k_i}{k} \tag{33}$$

$$\frac{C_g}{C}=\frac{1}{2}\left\{1+\frac{2k(h+\zeta)}{\sinh 2k(h+\zeta)}\right\} \tag{34}$$

Following Longuet-Higgins[1–6] the friction coefficient f_c is expressed by

$$f_c=\frac{2C_f H}{T\sinh k(h+\zeta)} \tag{35}$$

in which C_f is the non-dimensional friction coefficient and T is the wave period. For the turbulent viscosity, an empirical constant or the following equation is used.

$$A_l=\mu h \tag{36}$$

where μ is a constant. As the boundary condition, velocity, water elevation and surface flux are specified on the appropriate boundaries as follows.

$$u_i = \hat{u}_i, \quad \text{on} \quad S_1 \tag{37}$$

$$\zeta = \hat{\zeta}, \quad \text{on} \quad S_2 \tag{38}$$

$$\gamma_i = A_l(u_{i,j} + u_{j,i})n_j = \hat{\gamma}_i, \quad \text{on} \quad S_3 \tag{39}$$

where n_j denotes the components of the unit normals to the boundary and the circumflex denotes the prescribed value on the boundary.

FINITE ELEMENT METHOD

Basic equations for the analysis of the nearshore current are described in equations (13), (19), (25) and (26). It is notable that all these basic equations have the forms of the first order time dependent partial differential equation. For the discretization of the spatial unknown variables, the standard Galerkin finite element method has been successfully applied. The formulations are almost the same for all equations, i.e. those of wavenumber, wave energy and current flow. Assume that the flow field to be analysed is divided into small regions called finite elements. For the interpolation function, a linear polynomial function is used based on a triangular finite element.

For the computation of wave direction, equation (13) is employed. Multiplying both sides of equation (13) by weighting function k_i^* and integrating over the domain V, the weighted residual equation can be derived in the form:

$$\int_V \left(k_i^* \frac{\partial k_i}{\partial t}\right) \mathrm{d}V + \int_V (k_i^* C_{gj} k_{i,j}) \, \mathrm{d}V + \int_V (k_i^* f h_{,i}) \, \mathrm{d}V + \int_V (k_i^* k_j u_{j,i}) \, \mathrm{d}V + \int_V (k_i^* u_j k_{i,j}) \, \mathrm{d}V = 0 \tag{40}$$

The wavenumber k_i and its corresponding weighting function are interpolated in each finite element as follows.

$$k_i = \Phi_\alpha k_{\alpha i}, \qquad k_i^* = \Phi_\alpha k_{\alpha i}^* \tag{41), (42}$$

where Φ_α denotes the interpolation function, and $k_{\alpha i}$ and $k_{\alpha i}^*$ are nodal values of the wavenumber and the corresponding weighting function respectively. Water depth h, group velocity C_{gj}, current velocity u_i and gradient of frequency f are also interpolated as:

$$h = \Phi_\alpha h_\alpha, \qquad C_{gj} = \Phi_\alpha C_{g\alpha j} \tag{43), (44}$$

$$u_i = \Phi_\alpha u_{\alpha i}, \qquad f = \Phi_\alpha f_\alpha \tag{45), (46}$$

where h_α, $C_{g\alpha j}$, $u_{\alpha i}$, f_α are the nodal values of the corresponding variables at the αth node of each finite element. A standard linear interpolation function based on a three node triangular finite element is used. The Galerkin procedure leads, upon substituting equations (41)–(46) into equation (40), to the following finite element equation:

$$M_{\alpha\beta}\dot{k}_{\beta i} + K_{\alpha\beta\gamma j} C_{g\beta j} k_{\gamma i} + C_{\alpha\beta\gamma i} f_\beta h_\gamma + C_{\alpha\beta\gamma i} k_{\beta j} u_{\gamma j} + K_{\alpha\beta\gamma j} u_{\beta j} k_{\gamma i} = 0 \tag{47}$$

where

$$M_{\alpha\beta} = \int_V (\Phi_\alpha \Phi_\beta)\, dV$$

$$K_{\alpha\beta\gamma j} = \int_V (\Phi_\alpha \Phi_\beta \Phi_{\gamma,j})\, dV$$

$$C_{\alpha\beta\gamma i} = \int_V (\Phi_\alpha \Phi_\beta \Phi_{\gamma,i})\, dV$$

For the computation of wave height, equation (19) is employed. Multiplying both sides of equation (19) by weighting function E^* and integrating over the domain V, the weighted residual equation can be derived in the form:

$$\int_V \left(E^* \frac{\partial E}{\partial t}\right) dV + \int_V \{E^*[E(C_{gi} + U_i)]_{,i}\}\, dV + \int_V (E^* S_{ij} u_{i,j})\, dV = 0 \tag{48}$$

The wave energy E and its corresponding weighting function E^* are interpolated in each finite element as follows:

$$E = \Phi_\alpha E_\alpha, \qquad E^* = \Phi_\alpha E^*_\alpha \tag{49), (50}$$

where Φ_α denotes the interpolation function, and E_α and E^*_α are nodal values of wave energy and the corresponding weighting function, respectively. Radiation stress S_{ij} is also interpolated as:

$$S_{ij} = \Phi_\alpha S_{\alpha ij} \tag{51}$$

where $S_{\alpha ij}$ are the nodal values of the radiation stress at αth node of each finite element. The Galerkin procedure leads, upon substituting equations (44), (45), (49)–(51) into equation (48), to the following finite element equation.

$$M_{\alpha\beta}\dot{E}_\beta + B_{\alpha\beta i\gamma} E_\beta (C_{g\gamma i} + u_{\gamma i}) + C_{\alpha\beta\gamma i} E_\beta (C_{g\gamma i} + u_{\gamma i}) + K_{\alpha\beta\gamma j} S_{\beta ij} u_{\gamma i} = 0 \tag{52}$$

where

$$B_{\alpha\beta i\gamma} = \int_V (\Phi_\alpha \Phi_{\beta,i} \Phi_\gamma)\, dV$$

For the computation of nearshore current, equations (25) and (26) are employed. Multiplying both sides of equations (25) and (26) by weighting functions u^*_i and ζ^* and integrating over the domain V, the weighted residual equations can be derived in the form:

$$\int_V \left(u^*_i \frac{\partial u_i}{\partial t}\right) dV + \int_V (u^*_i u_i u_{i,j})\, dV + \int_V (u^*_i g \zeta_{,i})\, dV + \int_V \left\{u^*_i \frac{S_{ij,j}}{\rho(h+\zeta)}\right\} dV$$
$$+ \int_V \left\{u^*_i \frac{f_c}{(h+\zeta)} u_i\right\} dV + \int_V A_l (u^*_{i,j} u_{i,j})\, dV + \int_V A_l (u^*_{i,j} u_{j,i})\, dV = \int_{S_3} (u^*_i \hat{\gamma}_i)\, dS \tag{53}$$

$$\int_V \left(\zeta^* \frac{\partial \zeta}{\partial t}\right) dV + \int_V \{\zeta^*[(h+\zeta) u_i]_{,i}\}\, dV = 0 \tag{54}$$

Current velocity components u_i, water elevation ζ and their corresponding weighting

functions u_i^* and ζ^* are interpolated in each finite element as follows.

$$u_i = \Phi_\alpha u_{\alpha i}, \qquad u_i^* = \Phi_\alpha u_{\alpha i}^* \tag{55), (56}$$

$$\zeta = \Phi_\alpha \zeta_\alpha, \qquad \zeta^* = \Phi_\alpha \zeta_\alpha^* \tag{57), (58}$$

where Φ_α denotes the interpolation function. The radiation stress and bottom friction terms are interpolated as:

$$\frac{S_{ij}}{\rho(h+\zeta)} = \Phi_\alpha \left\{\frac{S_{ij}}{\rho(h+\zeta)}\right\}_\alpha \equiv \Phi_\alpha N_{\alpha ij} \tag{59}$$

$$\frac{f_c}{(h+\zeta)} u_i = \Phi_\alpha \left\{\frac{f_c}{(h+\zeta)} u_i\right\}_\alpha \equiv \Phi_\alpha F_{\alpha i} \tag{60}$$

where $N_{ij\alpha}$ and $F_{i\alpha}$ are the nodal values of the corresponding variables at the αth node of each finite element. The Galerkin procedures lead, upon substituting equations (43), (55)–(60) into equations (53) and (54), to the following finite element equations.

$$M_{\alpha\beta}\dot{u}_{\beta i} + K_{\alpha\beta\gamma j} u_{\beta j} u_{\gamma i} + H_{\alpha\beta i}\zeta_\beta + Q_{\alpha\beta j} N_{\beta ij} + M_{\alpha\beta} F_{\beta i} + S_{\alpha i\beta j} u_{\beta j} = 0 \tag{61}$$

$$M_{\alpha\beta}\dot{\zeta}_\beta + B_{\alpha\beta i\gamma}(h_\beta + \zeta_\beta) u_{\gamma i} + C_{\alpha\beta\gamma i}(h_\beta + \zeta_\beta) u_{\gamma i} = 0 \tag{62}$$

where

$$H_{\alpha\beta i} = \int_V (\Phi_\alpha \Phi_{\beta,i})\, \mathrm{d}V$$

$$Q_{\alpha\beta j} = \int_V (\Phi_\alpha \Phi_{\beta,j})\, \mathrm{d}V$$

$$S_{\alpha i\beta j} = \int_V A_l(\Phi_{\alpha,k}\Phi_{\beta,k})\delta_{ij}\, \mathrm{d}V + \int_V A_l(\Phi_{\alpha,i}\Phi_{\beta,j})\, \mathrm{d}V$$

Superposing equations (47), (52), (61) and (62) at all nodal points in the whole flow field, the final finite element equation can be derived as a non-linear first order simultaneous differential equation system. The finite element equations in the whole flow field can be written in the same form as in equations (47), (52), (61) and (62).

NUMERICAL INTEGRATION IN TIME

To solve the discretized finite element equations with appropriate initial and boundary conditions, a numerical integration scheme needs to introduced. For this purpose, the two step explicit scheme[14] is employed in this paper. The total time to be analysed is divided into a number of discrete time points, one of which is denoted by nth time point. The short time interval between the nth and $(n+1)$th time points is expressed by Δt. Applying the procedures to equations (47), (52), (61) and (62), the following two step scheme can be obtained denoting the values at the nth time point by superscript n.

Wave number

First step:

$$\bar{M}_{\alpha\beta} k_{\beta i}^{n+\frac{1}{2}} = M_{\alpha\beta} k_{\beta i}^n - \frac{\Delta t}{2}\left(K_{\alpha\beta\gamma j} C_{g\beta j}^n k_{\gamma i}^n + C_{\alpha\beta\gamma i} f_\beta h_\gamma + C_{\alpha\beta\gamma i} k_{\beta j}^n u_{\gamma j} + K_{\alpha\beta\gamma j} u_{\beta j} k_{\gamma i}^n\right) \tag{63}$$

Second step:

$$\bar{M}_{\alpha\beta}k_{\beta i}^{n+1} = M_{\alpha\beta}k_{\beta i}^{n} - \Delta t(K_{\alpha\beta\gamma j}C_{g\beta j}^{n+\frac{1}{2}}k_{\gamma i}^{n+\frac{1}{2}} + C_{\alpha\beta\gamma i}f_{\beta}h_{\gamma} + C_{\alpha\beta\gamma i}k_{\beta j}^{n+\frac{1}{2}}u_{\gamma j} + K_{\alpha\beta\gamma j}u_{\beta j}k_{\gamma i}^{n+\frac{1}{2}}) \tag{64}$$

Wave energy

First step:

$$\bar{M}_{\alpha\beta}E_{\beta}^{n+\frac{1}{2}} = M_{\alpha\beta}E_{\beta}^{n} - \frac{\Delta t}{2}(B_{\alpha\beta i\gamma}E_{\beta}^{n}(C_{g\gamma i} + u_{\gamma i}) + C_{\alpha\beta\gamma i}E_{\beta}^{n}(C_{g\gamma i} + u_{\gamma i}) + K_{\alpha\beta\gamma j}S_{\beta ij}^{n}u_{\gamma i}) \tag{65}$$

Second step:

$$\bar{M}_{\alpha\beta}E_{\beta}^{n+1} = M_{\alpha\beta}E_{\beta}^{n} - \Delta t(B_{\alpha\beta i\gamma}E_{\beta}^{n+\frac{1}{2}}(C_{g\gamma i} + u_{\gamma i}) + C_{\alpha\beta\gamma i}E_{\beta}^{n+\frac{1}{2}}(C_{g\gamma i} + u_{\gamma i}) + K_{\alpha\beta\gamma j}S_{\beta ij}^{n}u_{\gamma i}) \tag{66}$$

Nearshore current

First step:

$$\tilde{M}_{\alpha\beta}u_{\beta i}^{n+\frac{1}{2}} = \bar{M}_{\alpha\beta}u_{\beta i}^{n} - \frac{\Delta t}{2}(K_{\alpha\beta\gamma j}u_{\beta j}^{n}u_{\gamma i}^{n} + H_{\alpha\beta i}\zeta_{\beta}^{n} + Q_{\alpha\beta j}N_{\beta ij}^{n} + M_{\alpha\beta}F_{\beta i}^{n} + S_{\alpha i\beta j}U_{\beta j}^{n}) \tag{67}$$

$$\tilde{M}_{\alpha\beta}\zeta_{\beta}^{n+\frac{1}{2}} = \tilde{M}_{\alpha\beta}\zeta_{\beta}^{n} - \frac{\Delta t}{2}(B_{\alpha\beta i\gamma}(h_{\beta} + \zeta_{\beta}^{n})u_{\gamma i}^{n} + C_{\alpha\beta\gamma i}(h_{\beta} + \zeta_{\beta}^{n})u_{\gamma i}^{n}) \tag{68}$$

Second step:

$$\bar{M}_{\alpha\beta}u_{\beta i}^{n+1} = \bar{M}_{\alpha\beta}u_{\beta i}^{n} - \Delta t(K_{\alpha\beta\gamma j}u_{\beta j}^{n+\frac{1}{2}}u_{\gamma i}^{n+\frac{1}{2}} + H_{\alpha\beta i}\zeta_{\beta}^{n+\frac{1}{2}} + Q_{\alpha\beta j}N_{\beta ij}^{n+\frac{1}{2}} + M_{\alpha\beta}F_{\beta i}^{n+\frac{1}{2}} + S_{\alpha i\beta j}u_{\beta j}^{n+\frac{1}{2}}) \tag{69}$$

$$\bar{M}_{\alpha\beta}\zeta_{\beta}^{n+1} = \tilde{M}_{\alpha\beta}\zeta_{\beta}^{n} - \Delta t(B_{\alpha\beta i\gamma}(h_{\beta} + \zeta_{\beta}^{n+\frac{1}{2}})u_{\gamma i}^{n+\frac{1}{2}} + C_{\alpha\beta\gamma i}(h_{\beta} + \zeta_{\beta}^{n+\frac{1}{2}})u_{\gamma i}^{n+\frac{1}{2}}) \tag{70}$$

The overbar on the coefficient $\bar{M}_{\alpha\beta}$ expresses the lumped coefficient and $\tilde{M}_{\alpha\beta}$ is the selective lumping coefficient.

$$\tilde{M}_{\alpha\beta} = e\bar{M}_{\alpha\beta} + (1-e)M_{\alpha\beta} \tag{71}$$

where e is the parameter which represents the ratio of the lumped coefficient to the unlumped coefficient. This parameter e is referred to as the selective lumping parameter.

SOLUTION PROCEDURES

As was shown in the previous section, the basic equations of nearshore current can be divided into three parts, i.e. equations of wave direction, wave height and current flow. The most important procedure for the numerical integration in time is the selection of the time interval, which completely differs in each analysis of wave direction, wave height or current flow. It is almost impossible and also disadvantageous to solve parallelly all equations of wave and current. This is also due to the fact that the time scales of the phenomena are wholely different from each other.

The solution procedures used in the present computation are illustrated in Figure 2. First, the wave direction is solved by the kinematical conservation equation of wavenumber. Equations (63) and (64) are used, specifying the incidental wave direction on the oceanside boundary. As the initial condition, the wave directions at all nodal points in the whole field are assumed to be zero. Secondly, using the resulting wave direction, the wave height is derived from the conservation equation of wave energy. Equations (65) and (66) are employed, postulating the incidental wave height on the oceanside boundary. As the initial condition, the wave heights at all nodal points in the whole field are assumed to be zero. Thirdly, from the wave direction and wave height, the radiation stress which is the driving force of the current flow, can be obtained. The values of the radiation stress are computed at each nodal point using the values of wave direction and wave height at each nodal point. Finally, the nearshore current can be computed by the equation of momentum and the equation of continuity including the radiation stress. Equations (67)–(70) are used with appropriate boundary conditions for velocity, surface flux and water elevation. As the initial conditions, all nodal values of velocity and water elevation are supposed to be zero. The computation continues until the steady state has been reached. Because the equation system is non-linear, it is necessary to use iterative computation. Iteration has been performed independently for each stage of wave direction, wave height and current flow. First, the steady state of the wave direction is computed assuming the current velocity field. Secondly, the steady state of wave height is computed assuming wave direction and current flow. Then, the steady state of current flow is derived from the resulting wave direction and wave height. The iterative cycle is continued until convergence is obtained with respect to the current flow computed. For selective lumping parameter, $e = 0{\cdot}8$ was determined by several numerical experiments and used for all computations in this paper. All the computations for the flow have been carried out ignoring the radiation stress outside the surf zone, because the effect seems insignificant.

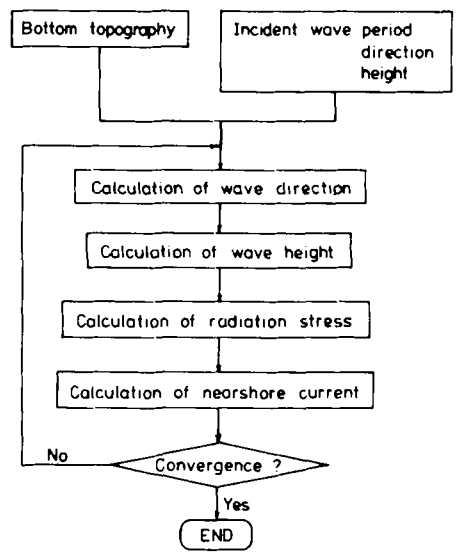

Figure 2. Flow chart

NUMERICAL TESTS

To show the validity of the present finite element method, several numerical computations have been carried out, of which results are compared with analytical solutions. For this purpose, numerical results are obtained by ignoring the coupling effect of current velocity. The first example is the computation of the refraction of waves compared with the Snell's law. Figure 3 shows the finite element idealizations and water depth employed in the comparative computation. The idealizations are named meshes A, B and C, respectively, as

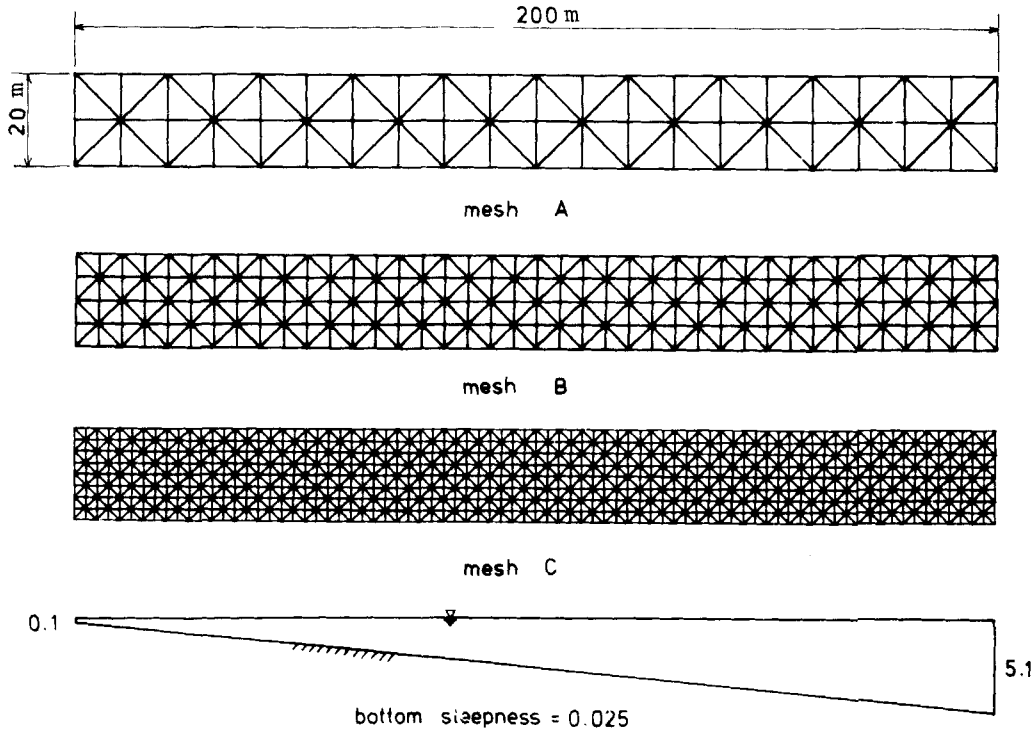

Figure 3. Finite element idealizations and water depth

the meshes are refined. The total numbers of finite elements and nodal points are listed in Table I. The period of the incident wave is taken as $T_0 = 10$ s. Figure 4 illustrates the computed wave angle compared with Snell's law. The computations have been carried out imposing various incident wave angles, using mesh B. The independent square marks in the Figure represent the computed wave angles, whereas the solid lines show those of the Snell's law. The wave angles computed by the present finite element method are well in agreement with those by the analytical methods. Figure 5 is the illustration of the comparison of the

Table I

	Total nodes	Total elements
mesh A	63	80
mesh B	205	320
mesh C	729	1280

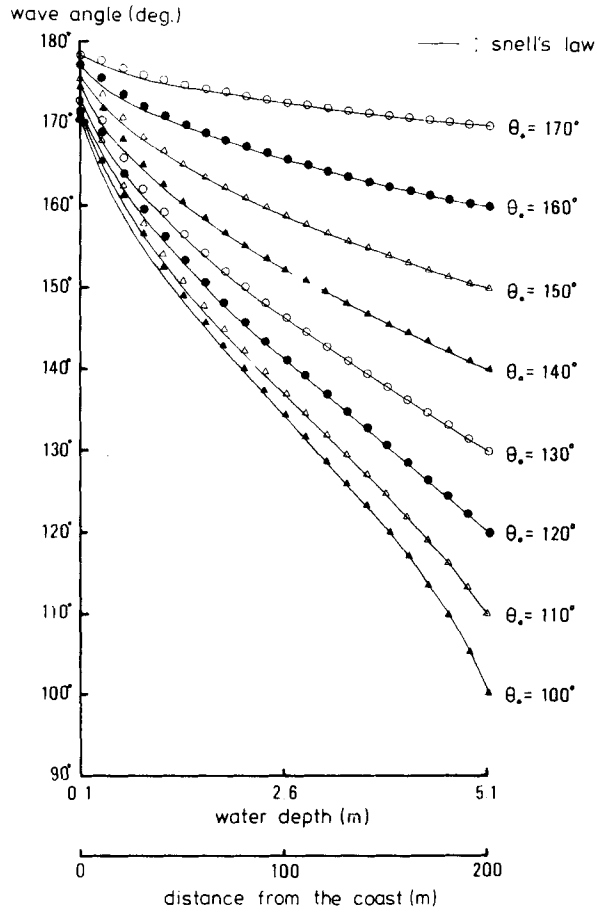

Figure 4. Computed wave angles using various incident waves

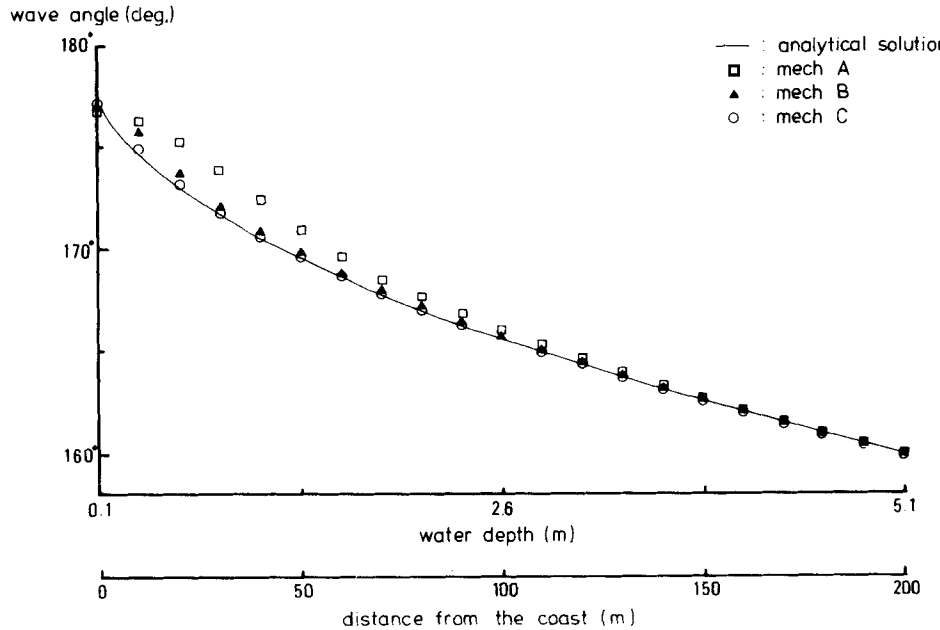

Figure 5. Computed wave angles based on various finite element idealizations

computed wave angles using various mesh refinements. This Figure shows that mesh B is sufficient for the computation of wave angle.

The second example is the comparison of wave height. Using the resulting wave angles, the wave height is computed, based on the various finite element refinements. The computed wave heights are plotted in Figure 6 with the analytical solution (solid line). Both numerical and analytical solutions are extremely well in agreement. In this example, mesh B is also sufficient to obtain reasonable numerical results.

The third example is the computation of the current flow in an idealized basin with an inclined coastline. Figure 7 shows the schematical illustration of the water tank used by Mizuguchi *et al.* to model experimentally the nearshore current flow.[15,16] The finite element idealization of the tank and the assumed water depth are represented in Figure 8. The total numbers of elements and nodes are 3369 and 1760. The computed wave angle and wavenumber are shown in Figure 9, in which inclination of arrow corresponds to wave angle, whereas length of arrow is wavenumber. At the offshore boundary, the incident wave angle is imposed to be perpendicular to the boundary, i.e. $\theta_0 = 270°$. The wave period is assumed to be $T_0 = 0{\cdot}71$ s. considering experiments. Figure 10 illustrates the computed wave height postulating that the incident wave height at the offshore boundary is $H_0 = 3{\cdot}8$ cm. The solid line shows the equiwave-height line. Both numerical results in Figures 9 and 10 were computed ignoring the coupling effect of current velocity. The current flow was obtained using the computed wave angle and height. On the coastal boundary, both components of velocity are assumed to be zero. Normal velocity to the boundary is taken as zero on the other three surrounding boundaries. For turbulent viscosity anf friction coefficient the values $A_l = \mu h$, $\mu = 0{\cdot}2$ and $C_f = 0{\cdot}02$ are employed. The computed current flow is shown in Figure 11. Comparison of the computed velocity with the analytical solution of Longuet-Higgins[5] is shown in Figure 12. The analytical solution is obtained by assuming a variable viscosity, which induces the discrepancy at the offshore coastal water. Considering this, the numerical and analytical solutions show reasonably good agreement.

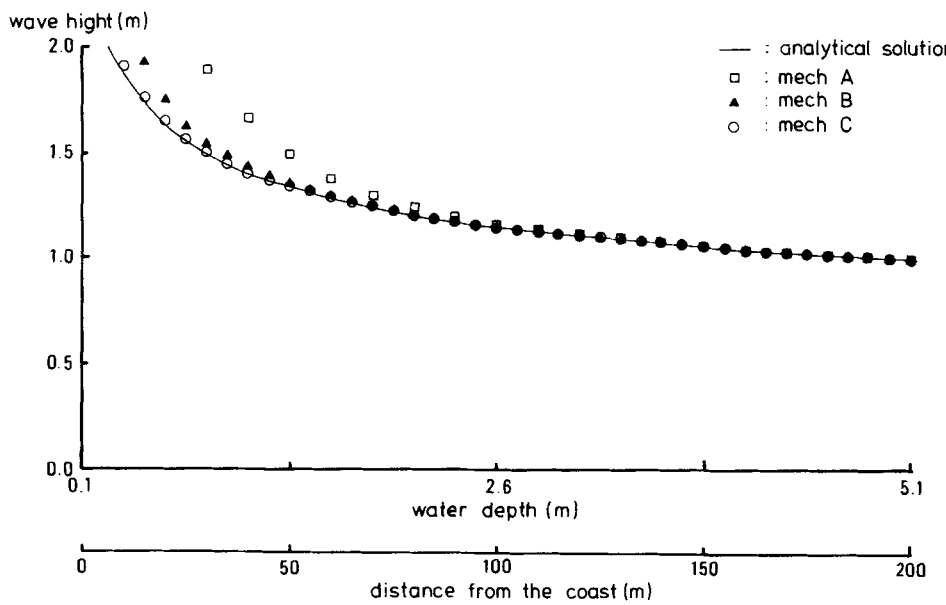

Figure 6. Computed wave heights based on various finite element idealizations

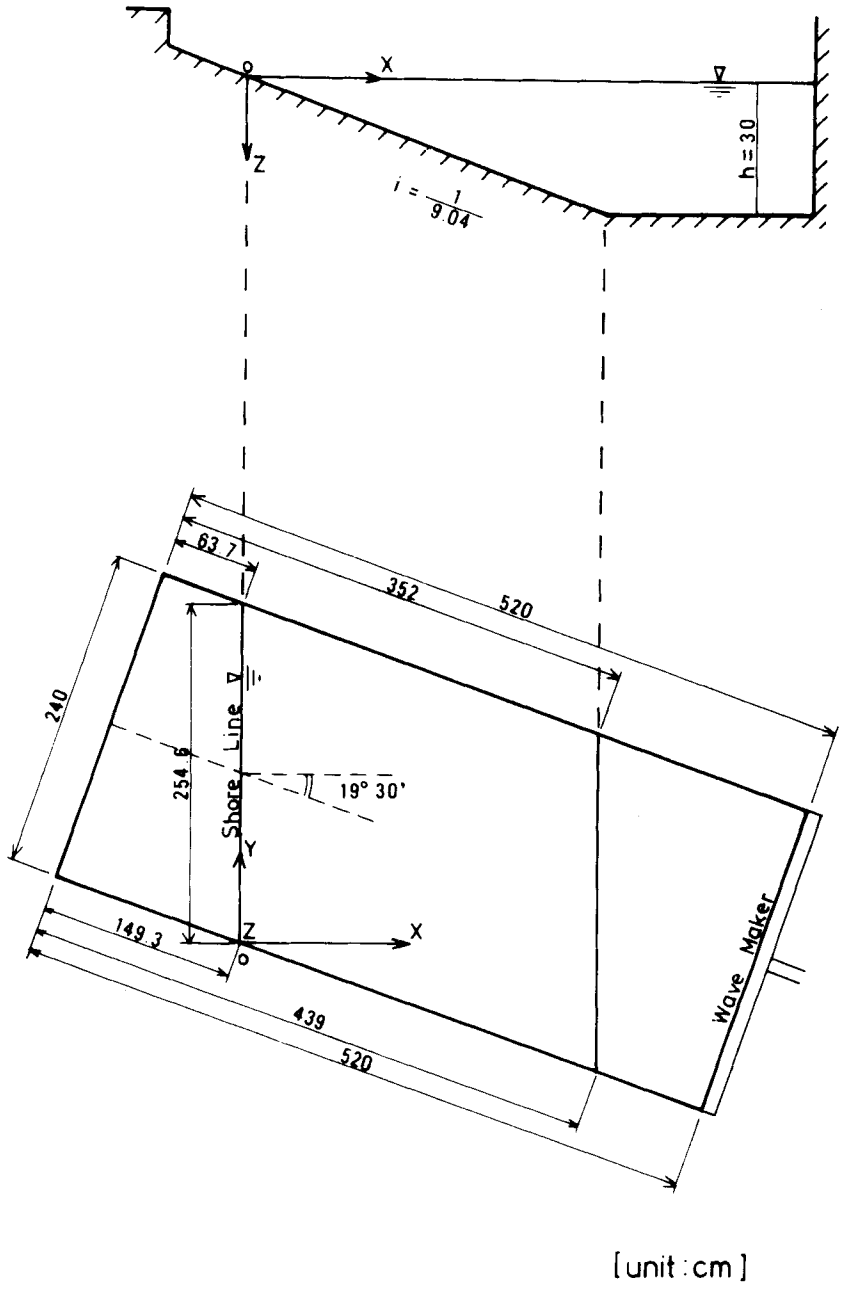

Figure 7. Outline of water tank

COMPARISON WITH EXPERIMENT

The numerical results by the present finite element method are compared with the experimental results of Mizuguchi *et al.*[15,16] The current flow shown in Figure 11 is employed for the computations of wave direction and wave height in the second cycle. The computed wave

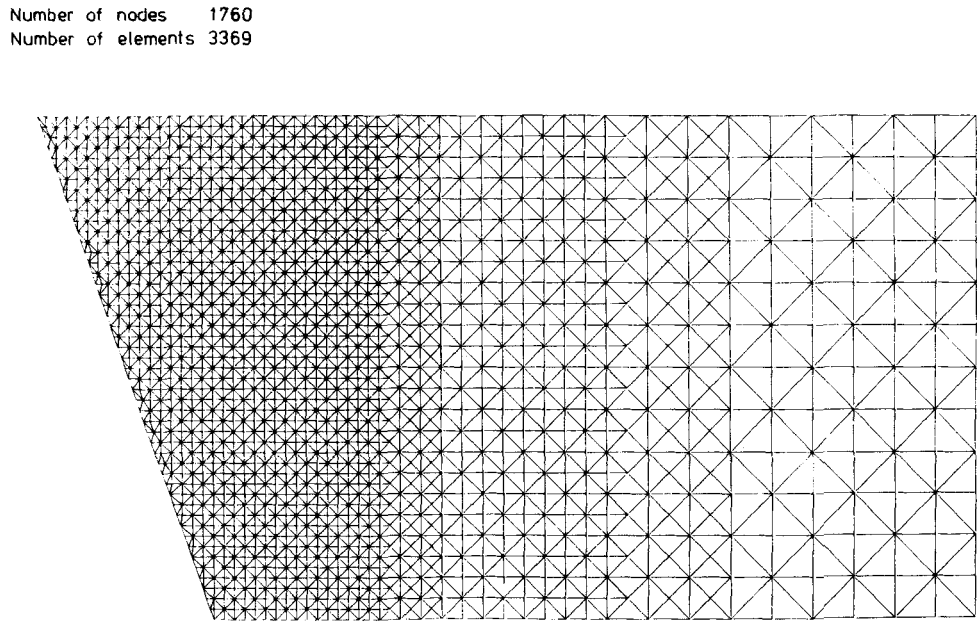

Figure 8. Finite element idealization of water tank

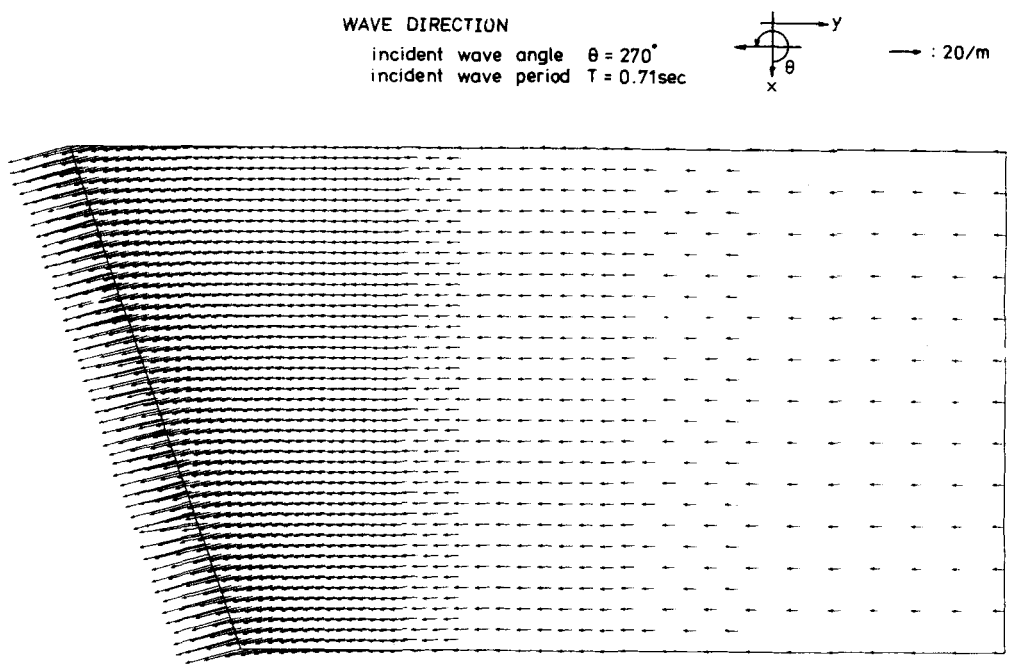

Figure 9. Computed wave direction without coupling of current

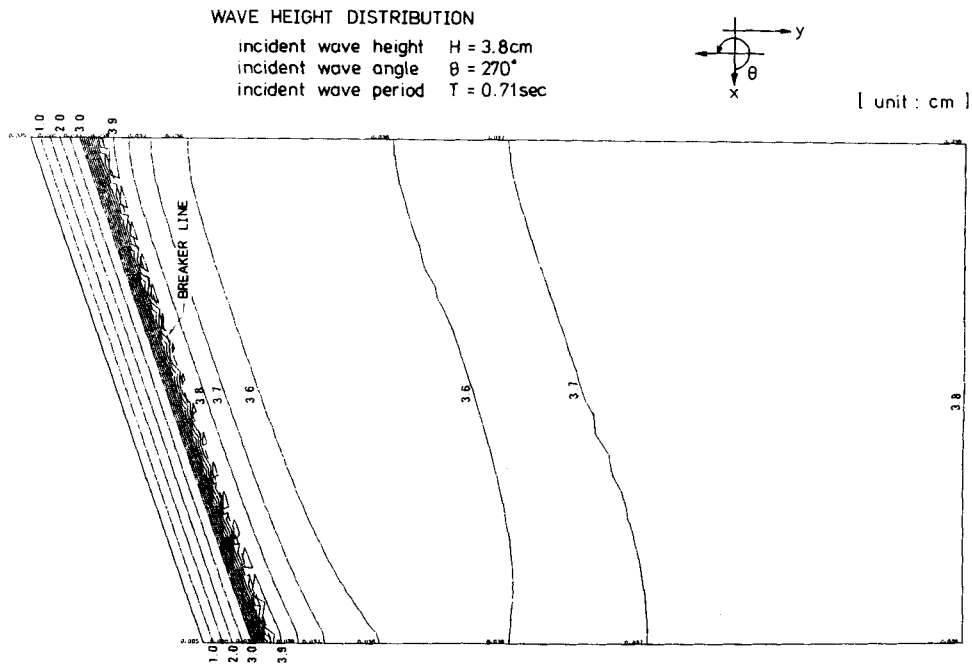

Figure 10. Computed wave height without coupling of current

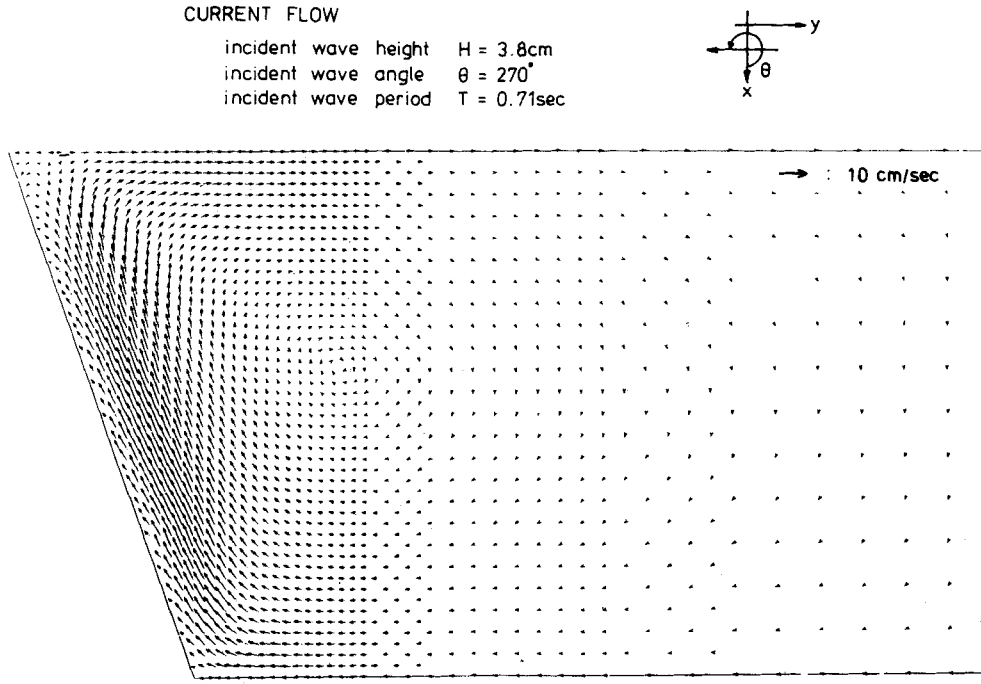

Figure 11. Computed nearshore current

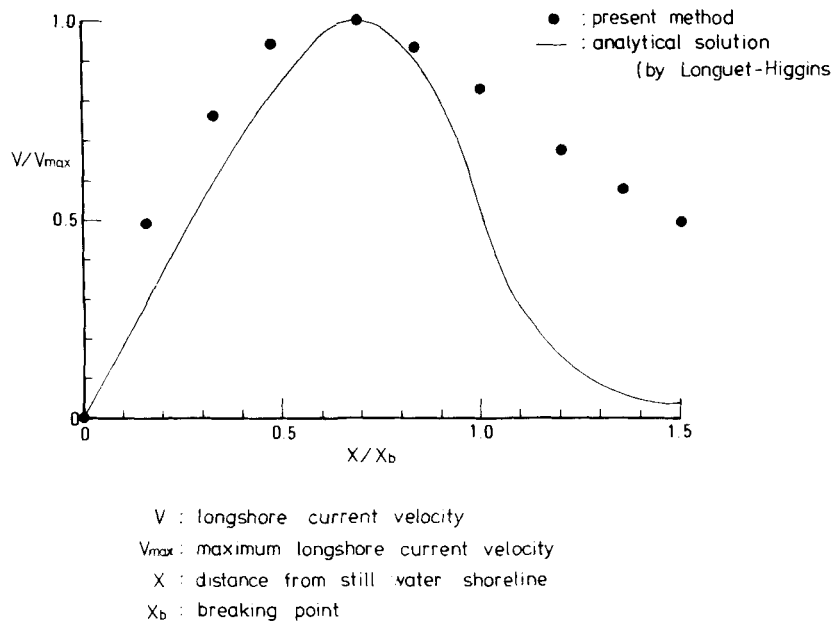

Figure 12. Comparison between numerical and analytical current velocities

angle and wavenumber are represented in Figure 13. Comparing Figure 13 with Figure 9, the indication that wave angle is affected by the current can be seen. Figure 14 is the representation of the computed wave height. The distribution of the wave height is affected by the current flow. In Figure 15, the computed current flow is represented. In Figure 16, comparison of longshore velocity with experiment is shown. White circles represent the experimental data, whereas black circles are the compuated data. Both observed and computed velocities are non-dimensionalized by the maximum values obtained. Comparison is carried out on the line $y = 135$ cm. If the computed results are shifted 10 cm to the shoreline side, both results are completely coincident. This is because the set up of the water elevation at the coastline was neglected in the computation. Figure 17 illustrates the comparisons of water elevation and wave height. Ignoring the set up at the coastline, both numerical and observed results are in extremely good agreement.

APPLICATION TO FUJISAWA COAST

The present finite element method is applied to the analysis of nearshore current on the Fujisawa coast in Japan. Along the coast, there is a natural sand beach, and no artificial structure is built around the area analysed. The local government has recently performed the observation of nearshore current. Figure 18 represents the finite element idealization for wave and current computations. The total numbers of finite elements and nodal points are 2928 and 1545, respectively. On the coastline, both components of velocity are specified as zero. On offshore and both side boundaries, normal velocity is assumed to be zero. The incident wave is imposed on the offshore boundary as wave angle $\theta_0 = 270°$, wave height $H_0 = 2$ m and wave period $T_0 = 10$ s. Figure 19 is the illustration of water depth and observed rip current zones. The contour lines represents the water depth, and the shaded zone shows the area in which the rip current is observed. The computation continued to the second

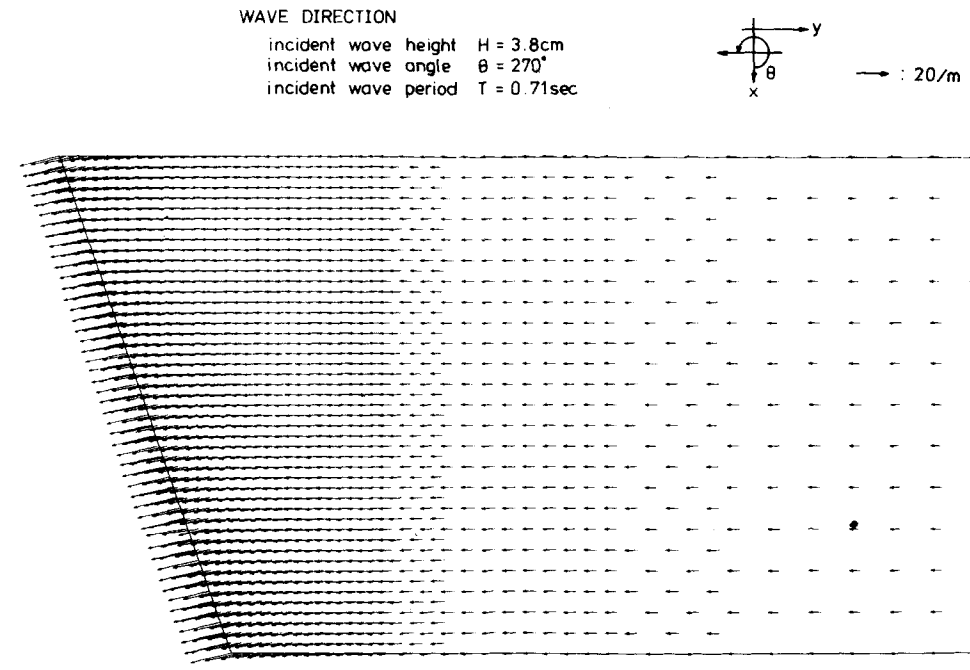

Figure 13. Computed wave direction coupling with current velocity

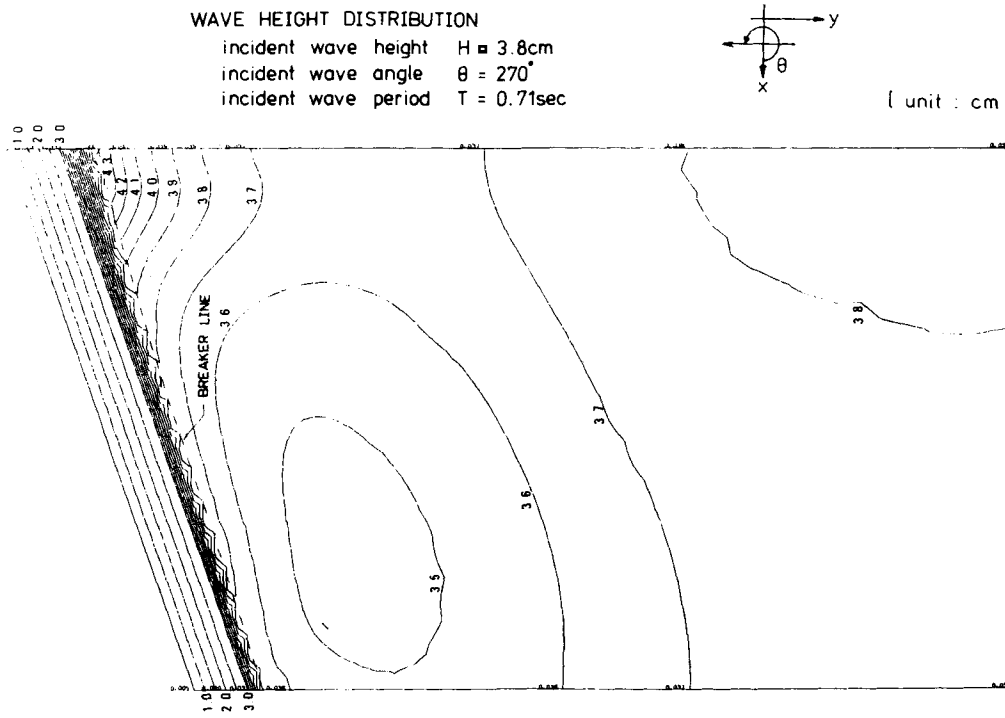

Figure 14. Computed wave height coupling with current velocity

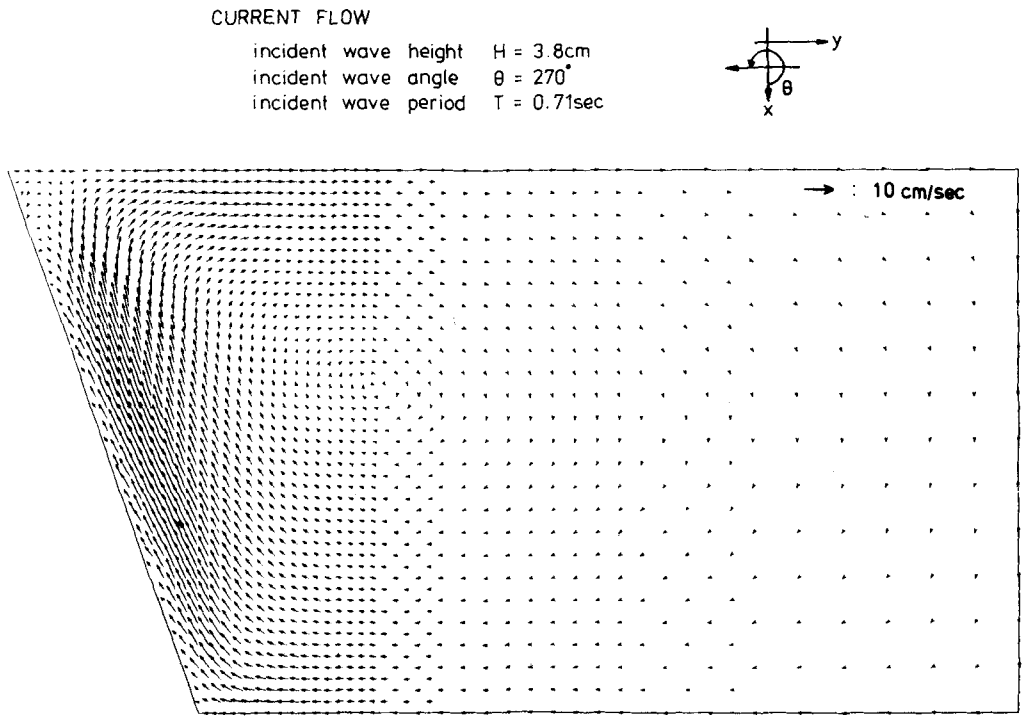

Figure 15. Computed nearshore current

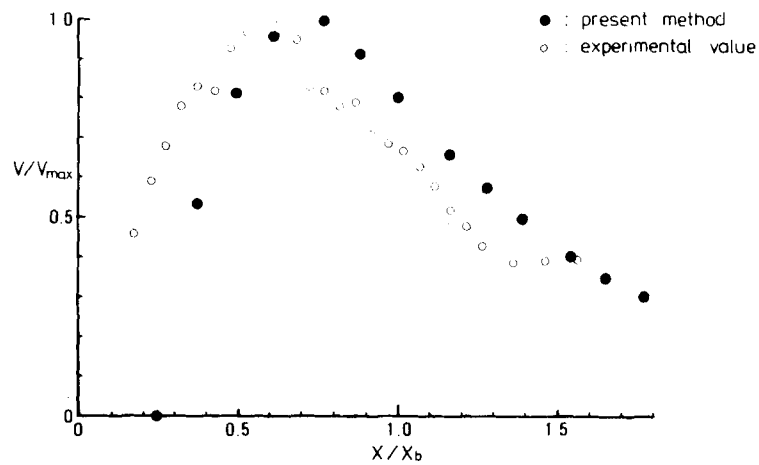

V : longshore current velocity
V_{max} : maximum longshore current velocity
X : distance from mean water shoreline
X_b : breaking point

Figure 16. Comparison between numerical and experimental velocity

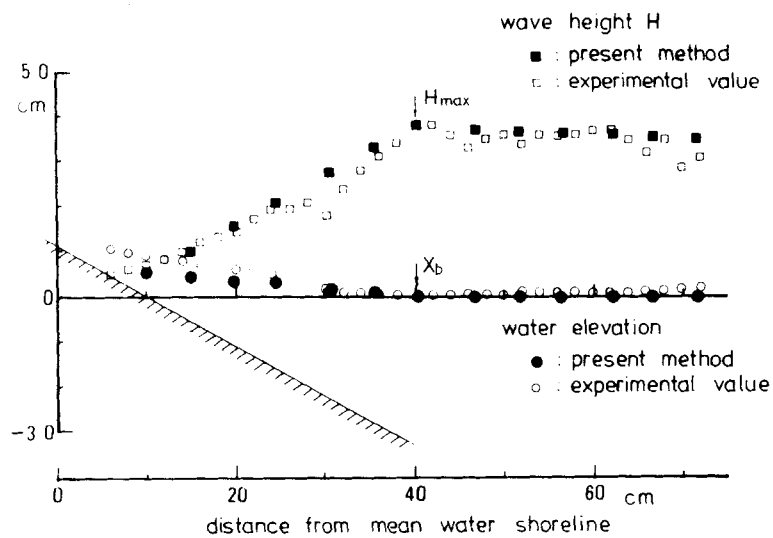

Figure 17. Comparison between numerical and experimental water elevation and wave height

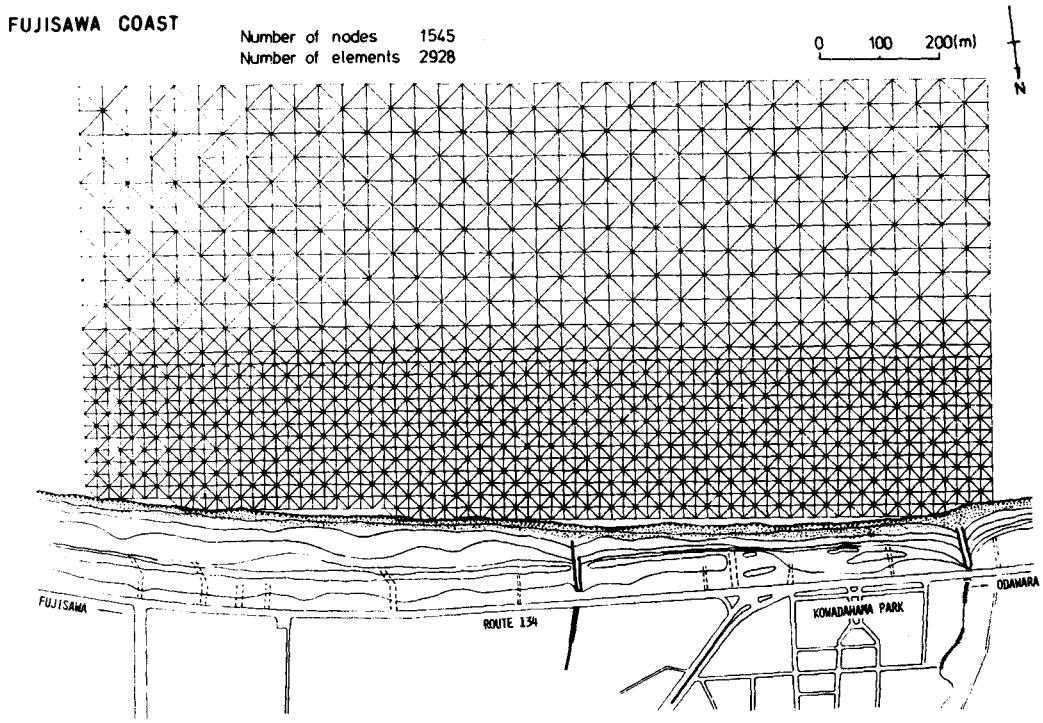

Figure 18. Finite element idealization of Fujisawa coast

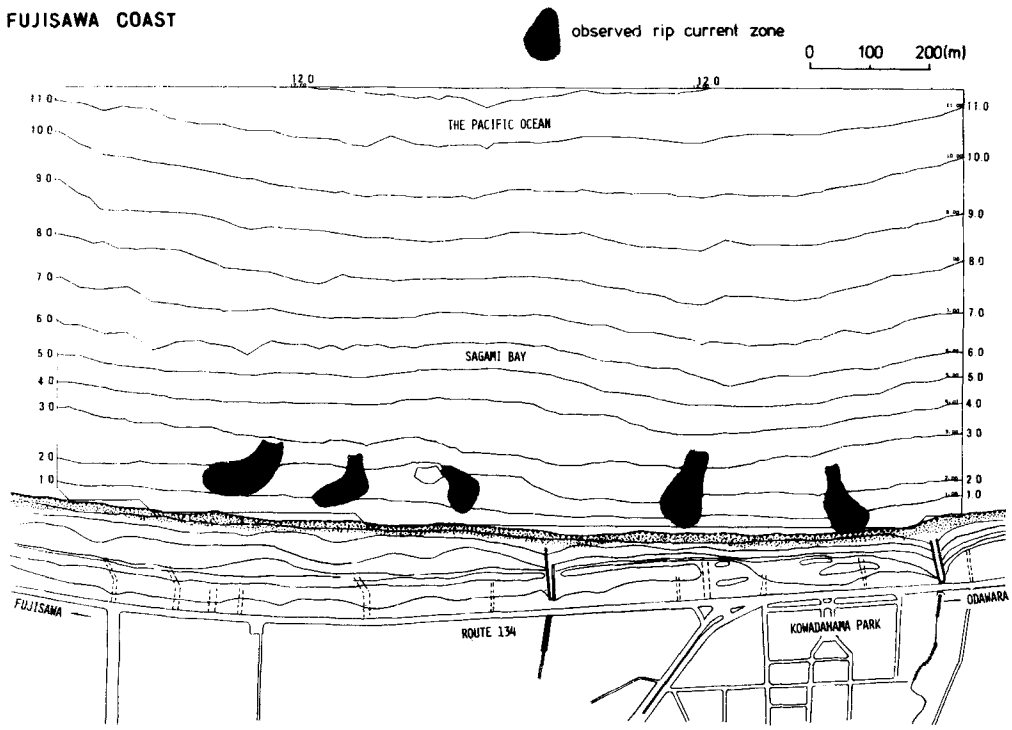

Figure 19. Water depth and observed rip current zone

iteration cycle. Namely, the computed wave direction and wave height are obtained by considering the coupling effect of current velocity. Comparing the computed velocity in the third iteration with that in the second iteration, it can be seen that the second iteration is sufficient to obtain the converged results. The wave angle and wave height are shown in Figures 20 and 21. The current flow is illustrated in Figure 22. Comparing the rip zones computed with those observed as in Figure 19, the locations of the zones are shown to be coincident. Figures 23 and 24 are the comparison of nearshore current according to the various incident wave directions and wave heights, respectively. In those Figures, it is seen that the nearshore current is extremely sensitive to the distribution of wave direction and wave height. For these computations of the current, eddy viscosity $A_l = 1{\cdot}0\ \mathrm{m}^2/\mathrm{s}$ and friction coefficient $C_f = 0{\cdot}02$ are employed. The time increment Δt is chosen to be 2·25 s.

CONCLUSION

The selective lumping two step explicit finite element method has been presented for the analysis of the transient nearshore current in a coastal sea. The present method is characterized by the following items. The first point is that the same solution procedures are used to determine the characteristics of wave and current. For this purpose, all basic equations are transformed into the form of the first order time dependent differential equation system. The second point is that a linear interpolation function based on a three node triangular finite element method is used for all field variables of wave direction, wave height, current velocity and water elevation. This allows use of the selective lumping two step explicit scheme for

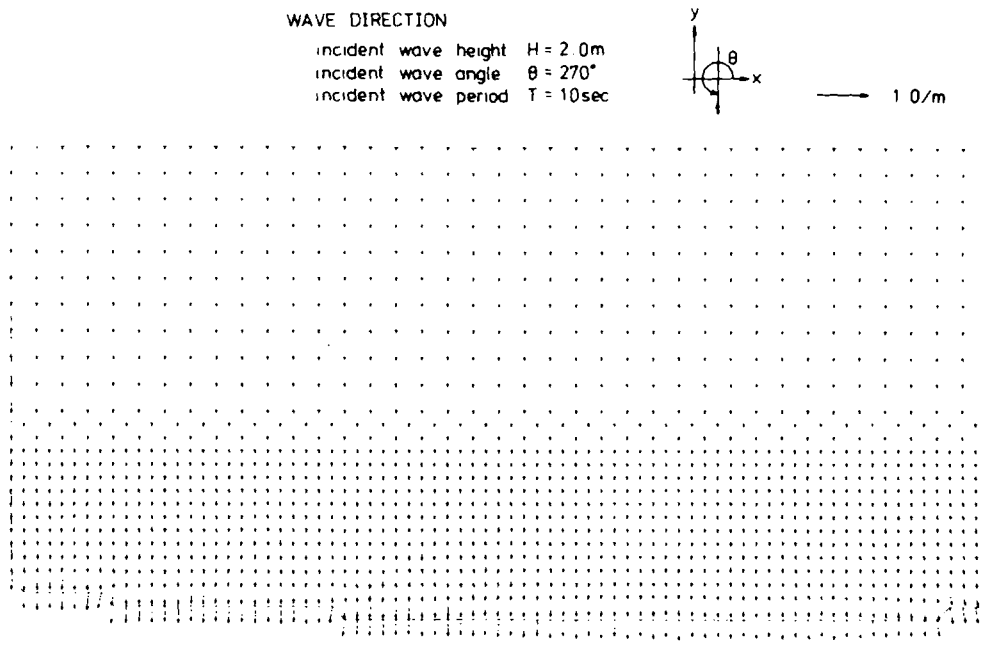

Figure 20. Computed wave angle at Fujisawa coast

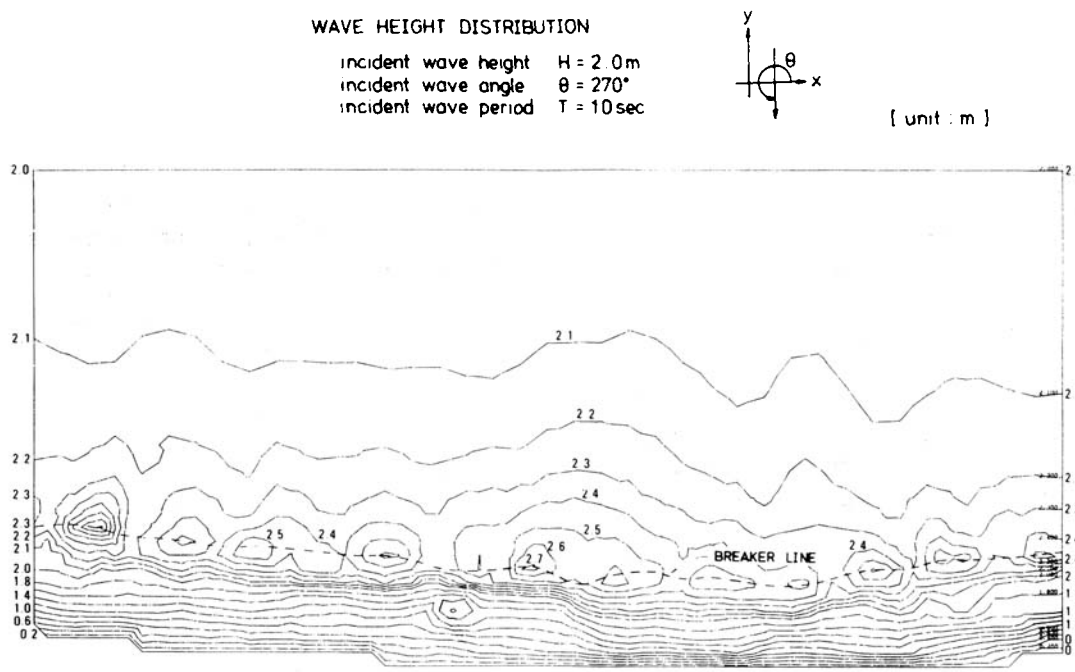

Figure 21. Computed wave height at Fujisawa coast

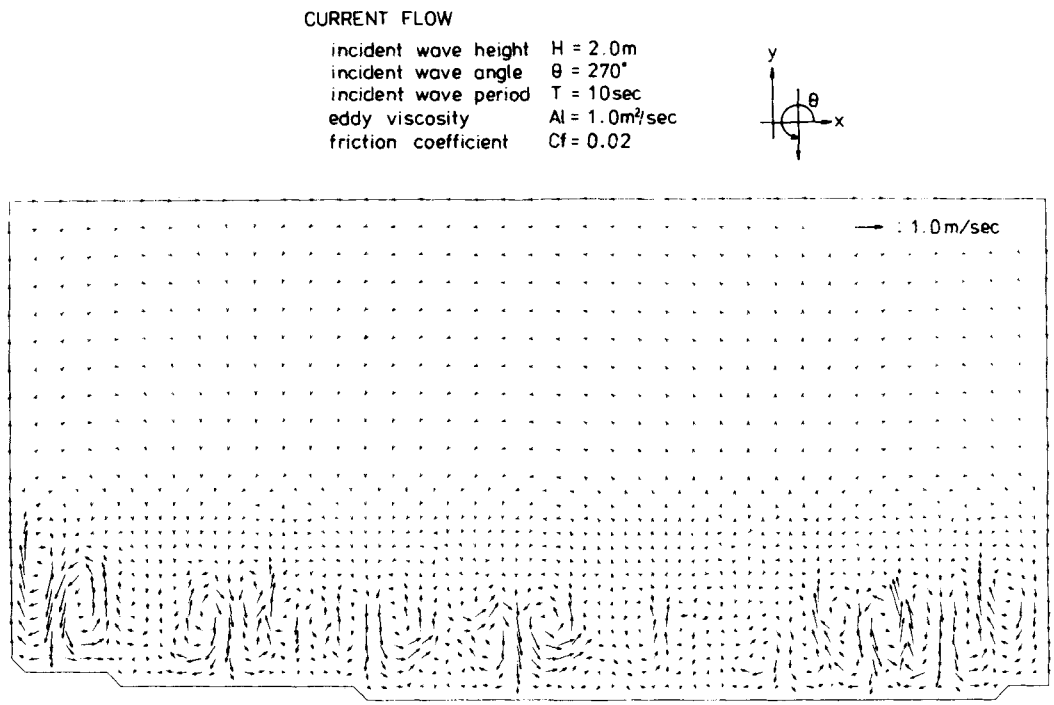

Figure 22. Computed nearshore current at Fujisawa coast with incident wave angle $\theta_0 = 270°$ and wave height $H_0 = 2{\cdot}0$ m

numerical integration in time, which is the third point. Finally, the computed results show extremely good agreement with analytical and experimental results. The water set up at the coastline which is ignored in this analysis ought to be considered. The computed flow patterns on the Fujisawa coast are in good agreement with the patterns observed. Thus, it is concluded that the present finite element method is extremely useful for the analysis of the nearshore current. The present procedures for wave analysis can be adapted for any natural coastal water. However, this method is not useful for the analysis of a water area including breakwaters such as harbours, ports, etc. because wave reflection and diffraction are not considered.

ACKNOWLEDGEMENT

The authors express their gratitude to Mr. Hirokazu Hirano, Mitsui Engineering & Shipbuilding Co., and Mr. Toshio Kodama, Graduate Student of Chuo University for their earnest discussions, and to Mr. Hirotsugu Nakashima and Mr. Atsushi Nakayama, Undergraduate Students of Chuo University for their help in making computer programs and performing computer runs. The computations in this paper have been carried out by FACOM M170F of Chuo University and HITAC M280H of the University of Tokyo. A part of this research is supported by a Grant in Aid in Engineering and Science, No. 56550319, Ministry of Education, Government of Japan.

The authors are also grateful for several valuable comments for future research by reviewers.

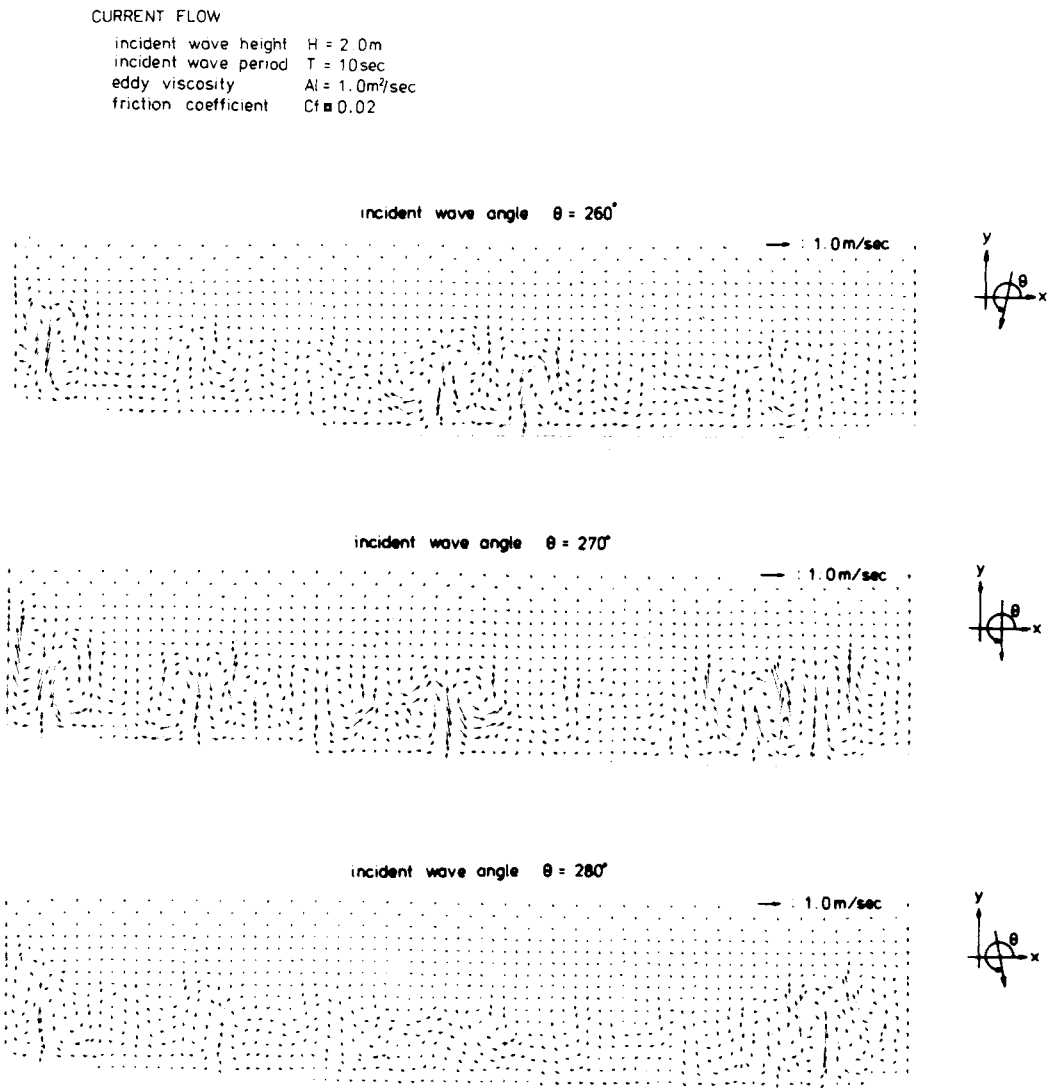

Figure 23. Computed nearshore current using various incident wave angles

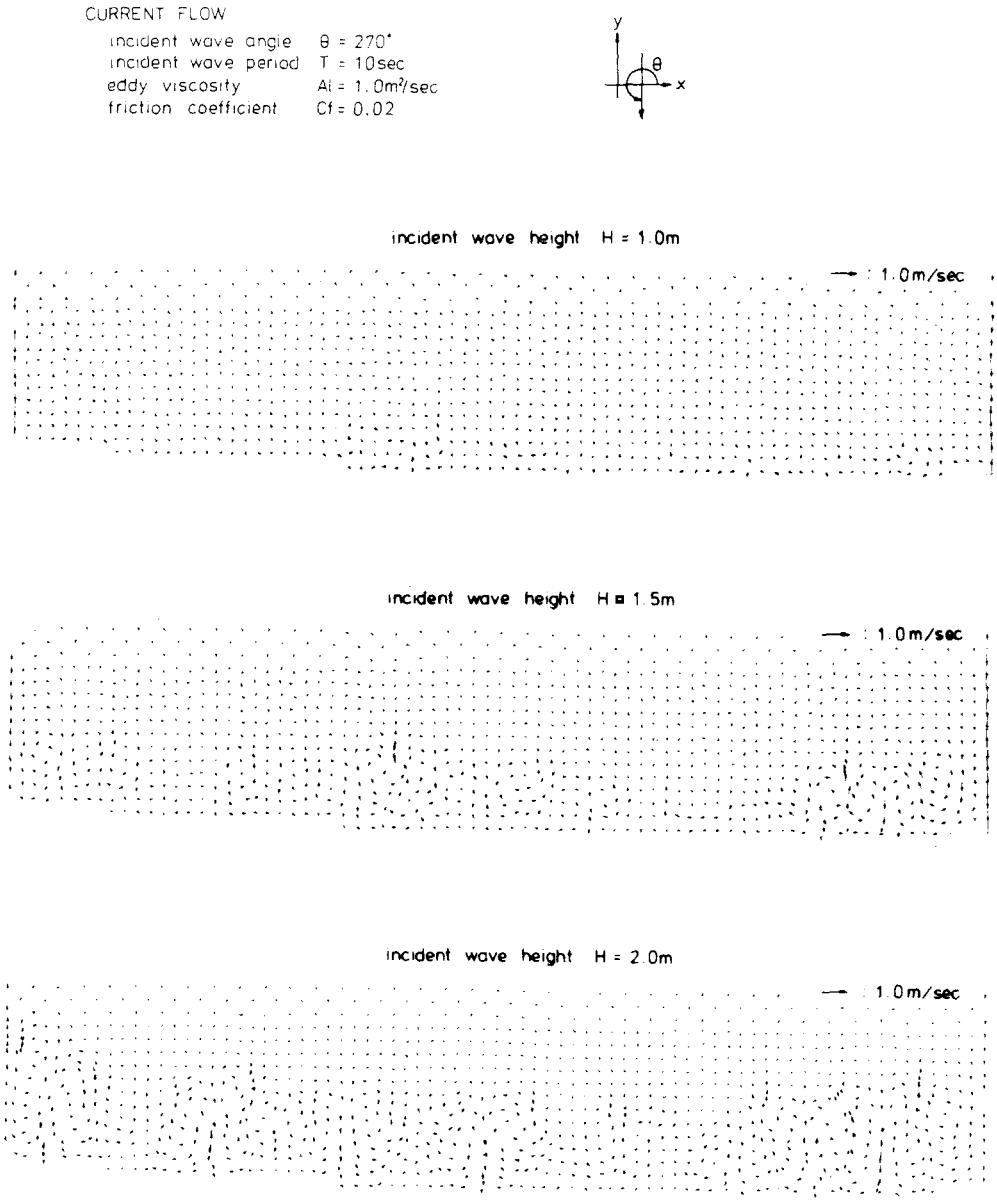

Figure 24. Computed nearshore current using various incident wave heights

REFERENCES

1. M. S. Longuet-Higgins and R. W. Stewart, 'Changes in the form of short gravity waves on long waves and tidal current', *J. Fluid. Mech.*, **8,** 565–583 (1960).
2. M. S. Longuet-Higgins and R. W. Stewart, 'The changes in amplitude of short gravity waves on steady non-uniform currents', *J. Fluid. Mech.*, **10,** 529–549 (1961).
3. M. S. Longuet-Higgins and R. W. Stewart, 'Radiation stress and mass transport in gravity waves, with application to surf beats', *J. Fluid. Mech.*, **13,** 481–504 (1962).
4. M. S. Longuet-Higgins and R. W. Stewart, 'Radiation stress in water waves: a physical discussion with applications', *Deep-sea Research*, **11,** 529–562 (1964).
5. M. S. Longuet-Higgins, 'Longshore current generated by obliquely incident sea waves, 1, 2', *J. Geophys. Res.*, **75,** 6778–6801 (1970).
6. O. M. Phillips, *The Dynamics of the Upper Ocean*, Cambridge University Press, 1977.
7. O. Skovgaard and I. G. Jonsson, 'Current depth refraction using finite elements', *Proc. Fifteenth Coastal Engineering Conference*, Honolulu, 1976, pp. 721–737.
8. P. L. Liu and G. P. Lennon, 'Finite element modelling of nearshore currents', *Proc. ASCE*, **104,** (WW2), 175–189 (1978).
9. P. Bettess, C. A. Fleming, J. C. Heinrich, O. C. Zienkiewicz and D. I. Austin, 'Longshore currents due to surf zone barrier', *Proc. Sixteenth Coastal Engineering Conference*, Hamburg, 1978, pp. 776–790.
10. C. S. Wu and P. L. F. Liu, 'Finite element modelling of breaking wave induced nearshore current', in Kawai (ed.) *Finite Element Flow Analysis*, 1982, pp. 579–586.
11. M. Kawahara, T. Takagi and K. Inagaki, 'A finite element method for nearshore current', *3rd Int. Conf. on Finite Element Method in Flow Problems*, Banff, 1980, pp. 70–79.
12. M. Kawahara and T. Takagi, 'Stream function finite elements for nearshore current', *Adv. Water Resourc.*, **5,** 195–207 (1983).
13. M. Kawahara, K. Kashiyama and Y. Irie, 'Finite element analysis of coastal process', in Kawai (ed.) *Finite Element Flow Analysis*, 1982, pp. 571–578.
14. M. Kawahara, H. Hirano, K. Tsubota and K. Inagaki, 'Selective lumping finite element method for shallow water flow', *Int. J. Num. Meth. Fluids*, **2,** 89–112 (1982).
15. M. Mizuguchi, K. Kobayashi, M. Okuyama and Y. Morita, 'Experimental study of the influence of the bottom roughness on the longshore current', *Bull. Fac. Sci. and Engng., Chuo University*, **22,** 205–219 (1979).
16. M. Mizuguchi and K. Horikawa, 'Experimental study on longshore current velocity distribution', *Bull. Fac. Sci. and Engng., Chuo University*, **21,** 123–150 (1976).
17. Government of Kanagawa prefecture, 'Report on investigation for protection of coastal erosion', 1971 (in Japanese).